Research Article Vol. 57, No. 14 / 10 May 2018 / Applied Optics 3953

applied optics

3D-printed polymer antiresonant waveguides for short-reach terahertz applications

L. D. van Putten,[1,*] J. Gorecki,[1] E. Numkam Fokoua,[1] V. Apostolopoulos,[2] and F. Poletti[1]

[1]Optoelectronics Research Centre, University of Southampton, SO171BJ Southampton, UK
[2]School of Physics and Astronomy, University of Southampton, SO171BJ Southampton, UK
*Corresponding author: ldvp1g13@soton.ac.uk

Received 23 January 2018; revised 30 March 2018; accepted 31 March 2018; posted 3 April 2018 (Doc. ID 320397); published 10 May 2018

In this work, we present a 3D-printed waveguide that provides effective electromagnetic guidance in the THz regime. The waveguide is printed using low-cost polycarbonate and a conventional fused deposition modeling printer. Light guidance in the hollow core is achieved through antiresonance, and it improves the energy effectively transported to the receiver compared to free space propagation. Our demonstration adds to the field of 3D-printed terahertz components, providing a low-cost way of guiding terahertz radiation.

OCIS codes: (230.7370) Waveguides; (060.2280) Fiber design and fabrication; (060.2310) Fiber optics; (300.6495) Spectroscopy, terahertz.

https://doi.org/10.1364/AO.57.003953

1. MOTIVATION

THz spectroscopy grew significantly during the 1990s and is inexorably linked with the invention of the Terahertz Time-Domain Spectrometer (THz-TDS). Auston *et al.* in 1984 [1] demonstrated the generation of freely propagating broadband, single-cycle THz pulses from photoconductive antennas. These sources, in combination with pulsed lasers, directly led to the realization of the THz-TDS. This arrangement employs a synchronous detection scheme resembling a pump-probe setup with an inherent high signal-to-noise ratio, which allows for accurate measurements. Some notable characteristics of THz-TDS are that it gives a complete solution for measurements in the THz range, where the electric field in time is measured, and also frequency information can be obtained using a fast Fourier transform. The obtained spectrum range from a THz-TDS spans multiple octaves, usually from 50 GHz up to 3 THz. Due to the synchronous detection, THz-TDS allows pulses with energy below the black-body radiation to be measured, as thermal radiation will average to zero; thus high signal-to-noise ratios can be achieved, equivalent to synchrotron sources [2]. Furthermore, rather than the intensity of the signal, transient electric fields are measured using THz-TDS, and thus the measurement can reveal unambiguously the complex permittivity of the investigated sample without having to use the Kramers–Kronig relations [3,4]. Waveguides for the terahertz regime could be used for microscopy, terahertz quantum-cascade lasers, and imaging [5], but could also be useful in spectroscopy applications to replace complicated lens systems. Besides, data transmission systems in the THz range might benefit from a reliable waveguide signal delivery system. Terahertz waveguides and fibers allow for a terahertz pulse to be delivered to remote locations in environments that may be hostile or hazardous, and for efficient coupling between components such as emitters and detectors. THz waveguides have been demonstrated for industrial monitoring of chemical reactions by measuring ammonium chloride aerosol by-products [6], for probing pharmaceuticals such as aspirin [7], and for suggested uses in medical endoscopy of internal organs by utilizing flexible waveguides [8].

To be able to use the terahertz part of the spectrum to transmit data as currently is done at microwave and optical frequencies, it is essential to be able to design and produce critical devices such as couplers, waveguides, lenses, and gratings [9,10]. Since 2015, demonstrations have started to emerge of the fabrication of THz components via 3D printing, creating structures with macroscopic anisotropy owing to material filament widths of a similar order of scale to terahertz wavelengths [6,11]. The development of a wide range of these components could allow for bespoke multicomponent THz systems to be printed as a single part.

A challenge in the design of a waveguide for the terahertz regime lies in the high material absorption for these frequencies [12]. One of the materials operating in this region is TOPAS, where at 1 THz the transmission loss is still over 2 dB/cm [12]. Hollow-core fibers have great potential in the terahertz regime,

as the light mainly propagates in an air core, with a relatively low fraction of the field being confined in a solid material [12]. Different guiding mechanisms can be exploited for guidance in a hollow-core fiber [13,14]. Two common single-material hollow-core fibers exploit guidance through the photonic bandgap (PBG) or use of antiresonances (AR) in the core surround [15]. Out of many ways to fabricate these waveguides, recent attention has been directed towards 3D printing. There are different types of 3D printing. Different polymer THz waveguides designs have been produced using a variety of 3D printing methods [5,11,16–18]. However, the designs of these waveguides require very small features, which can only be obtained with expensive laser-based 3D printing techniques. The cheaper 3D printing version, Fused Deposit Modeling (FDM) printing would not be able to produce such small details, since the smallest feature that can be printed is dependent on the nozzle size and is typically larger than the cone tip [16]. In this work, we demonstrate that an FDM printer can also be employed to produce a useful THz waveguide.

Jahn *et al.* [9] have designed and fabricated a focusing grating coupler for the terahertz regime using FDM 3D printing of a polystyrene filament. However, due to the design in this component, the beam is only focused in one direction, creating an oval shaped focal spot. A 3D-printed "quasi-Wollaston-prism" has been demonstrated for THz applications via the FDM printing method where macroscopic birefringence is produced via manufacturing a grid-like structure [17]. The component allows for two orthogonally polarized beams to be split, achieving a separation angle of 23°. They also demonstrated a 3D-printed THz q-plate [18] to generate cylindrical vector beams. Waveguides for the terahertz regime have also been manufactured using 3D printing, including hollow-core waveguides [19,20].

In this work, we design and fabricate a polymer hollow core waveguide that can be produced using any commercially available FDM printer. FDM printed waveguides could provide a quick solution for aligning and focusing terahertz waves, and also could be customized to each application due to the flexibility in the design and fabrication process. In this work, we have fabricated an AR waveguide for the terahertz regime, with a cladding design using half-elliptical cladding elements, that has recently been demonstrated able to minimize the required structural dimension for a desired value of loss [21].

2. WAVEGUIDE DESIGN AND FABRICATION

In a hollow-core AR fiber, light is confined and guided in the air core by virtue of the resonant reflection provided by thin membranes that surround it and behave effectively as a Fabry–Perot cavity. The transmission properties of such a waveguide therefore depend on the thickness of these membranes and on the properties of the material of which they are made, specifically its refractive index. The transmission spectrum of such an AR waveguide consists of windows of high transmission and low loss (AR windows), separated by low transmission and high loss peaks at frequencies that are resonant within the membranes (see Fig. 1). The frequencies where resonance occurs can be calculated using

$$f_{\mathrm{mres}} = c * \left(\frac{2t}{m}\sqrt{n^2 - 1}\right)^{-1}, \tag{1}$$

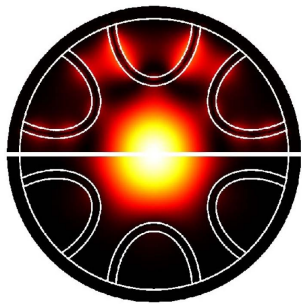

Fig. 1. Mode profile at (top) resonance, 0.3 THz, and (bottom) antiresonance, 0.2 THz.

where c is the speed of light, n is the refractive index of the material the AR waveguide is made of, t the element thickness of the structure in the cladding, and m is an index annotating the different resonant frequencies.

As our waveguides are fabricated using an FDM printer, the thickness of the membrane in the cladding depends on the nozzle size of the printer. For the printer available to us, the UP 2 Plus Printer from UP3D, the thickness of the membranes that can be produced is limited to multiples of 0.6 mm. We are using polycarbonate, of which the refractive index in the terahertz range is 1.6 [22]. A thickness of 0.6 mm fixes the position of the first four resonances at 0.2, 0.4, 0.6, 0.8 THz. A different nozzle would be required to print membranes of different thickness and shift the resonance peaks. The cladding design used in the waveguides reported in this paper consists of semi-elliptical membranes, which have been shown to offer low loss at optical frequencies [21]. We designed and fabricated three different waveguides, the parameters of which are shown in Table 1.

Finite element simulations (using the commercial FEM solver COMSOL Multiphysics) were performed for each of the three designs to study theoretically their transmission characteristics. Loss in these waveguides is dominated by leakage since only a very small fraction of light, less than 0.1% at antiresonance, propagates in the solid material. The calculated loss spectra for each of these waveguides are shown in Fig. 2. Design C has twice as many resonance peaks as designs A or B, since its membranes are twice as thick. Design A shows higher transmission losses because of its smaller core size: loss in these waveguides is found to scale approximately as $\frac{\lambda^2}{r^4}$ [23]. This can also be seen in Fig. 2, as the loss decreases with increasing frequency. In waveguide B, there exists some frequencies (e.g., 0.36 THz) where the loss (0.009 dB/cm) is over 2500 times lower than the material loss [12,15], showing that the hollow-core waveguide can be effective in guiding THz radiation. The antiresonance in the waveguide design makes the waveguide suitable to guide

Table 1. Parameters for Designed Waveguides as Shown in Fig. 3

	Thickness (t) (mm)	Core Size (d) (mm)	Ellipse Length (mm)
A	0.6	6	3.6
B	0.6	10	5
C	1.2	10	5

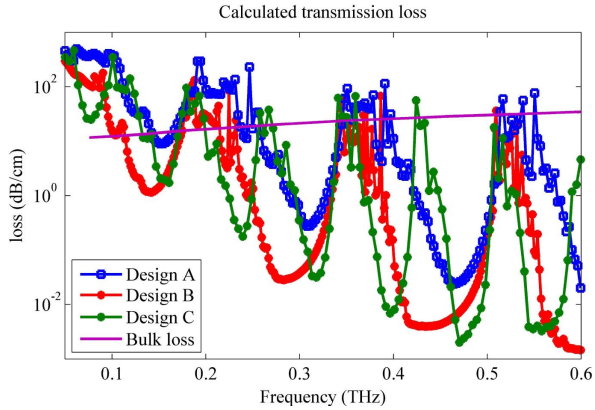

Fig. 2. Simulation results for transmission loss for all three waveguides compared to the bulk loss of polycarbonate.

certain frequency bands, and less suitable for frequencies where there is resonance. To achieve guidance at different frequencies, a different thickness of the cladding elements is needed to shift the resonance peaks. The loss at resonance frequencies can be higher than the bulk loss of the material the cladding is made of, as the loss is dependent on the structure of the cladding elements.

It can be seen from Fig. 2 that design B combines the lowest transmission losses, and the broadest bandwidth. These three designs were manufactured out of polycarbonate using our 3D printing method. Polycarbonate is suitable as a material for the AR waveguide due to the low absorption of terahertz (of the order of 10s of dB/cm) compared to other polymers [12], and is readily available as filament for an FDM printer. Although there are materials with lower absorption in the terahertz regime, for example Cytop and Zeonex [12], no readily available printing filaments can be found to date for these materials.

3. EXPERIMENTAL SETUP AND RESULTS

To test the guidance and transmission of the three waveguides, the TDS setup in Fig. 3(a) is used. To ensure that the amount of input coupled light is similar for all measurements, the waveguides are held in the setup using a thin metal disk with an aperture in the center corresponding with the core size of the waveguides, as shown on the right in Fig. 3(b). The terahertz emitter is Tera-SED from Laser Quantum GMBH, a GaAs photoconductive emitter that emits broadband terahertz waves up to 2.5 THz [24]. The detector used is a Menlo GMBH TERA8-1 photoconductive antenna [25] that has a bandwidth of up to 4 THz. Although the emitter and detector are active up to 2.5 THz and 4 THz, respectively, the spectroscopic bandwidth is limited by ambient noise and component alignment, with the latter having greater effect at higher frequencies. The resultant effective bandwidth over which useful spectroscopic data can be obtained is in the range of 0.1 THz to 1.0 THz. In the setup, we tried to minimize the distance between the waveguide and detector/emitter, so that at both ends of the waveguide we had about a 6 mm gap. All three waveguides are 8.7 cm in length, and the emitter

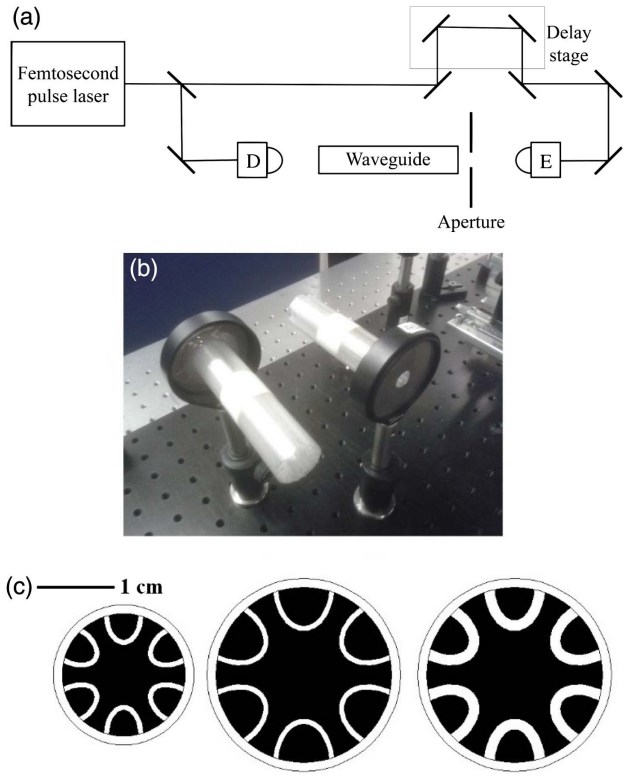

Fig. 3. (a) Systematic overview of THz-TDS spectroscopy setup. Detector (D) from [25] and emitter (E) from [24], both photoconductive antennas and mounted with silicon lenses. (b) Metal disks shown with waveguides to aid alignment. (c) All three designs shown on scale.

and detector were not moved during the transmission measurement. In Fig. 3(c) a cross section of each design is shown.

For each waveguide, the transmission spectrum is measured using TDS. This measurement is repeated five times for each waveguide and is normalized using a reference scan. The reference scan is taken without a waveguide in place, while keeping the metallic disk aperture in the setup and the distance between the detector and emitter the same. The frequency domain data for these measurements is shown in Fig. 4. The raw time-domain data can be found in [26]. The data from these transmission measurements is normalized to the measured loss without waveguide or aperture present in the setup (i.e., free space propagation). The results for the normalized transmission can be seen in Fig. 5.

First of all, it can be seen that there are spectral regions where the normalized transmission is higher than 1, showing that the waveguides are guiding in the antiresonance regions. This means that for terahertz setups, a 3D-printed waveguide could provide a quick and cheap alternative to complicated lenses systems that are sensitive to alignment. Besides, for waveguide A and B, the measured spectral position of the resonances (dips in the transmission spectrum, where little light propagates) agree fairly well with the expected values (red lines). For waveguide C, where it is expected to have resonances at the same frequencies as well as additional resonances in between, the resonances are less apparent in the measurements.

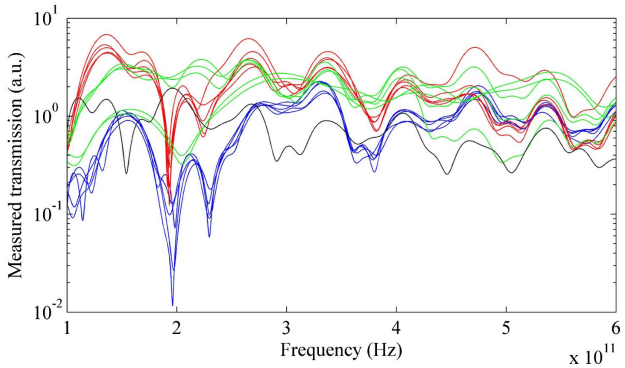

Fig. 4. Transmission measured for each waveguide (blue A, red B, green C) and for the reference scan (black)—displayed in frequency domain.

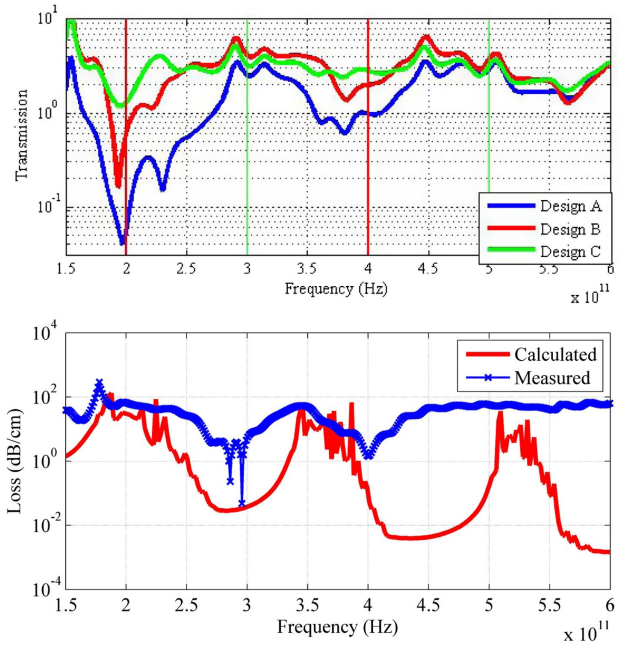

Fig. 5. (top) Transmission measured for each waveguide. The transmission is normalized using a reference scan without a waveguide in the setup. Red vertical lines indicate expected resonances (high loss, transmission dips) for all three waveguides; green lines indicate additional expected resonances for waveguide C. (bottom) Calculated loss and measured loss for waveguide B and bulk loss for polycarbonate compared.

We believe that this might be due to the way the double thickness layer is printed, which leads to significantly more deviations in the width of each cladding element, and possibly even air gaps in between the two adjacent layers. These air gaps could be affecting the transmission in the waveguide and also result in a change in the thickness of the cladding structure compared to the design, which will alter the antiresonance frequencies. For an effective AR 3D-printed waveguide, it would be better to adjust the nozzle size such that the required element thickness is achieved from a single pass of the printer.

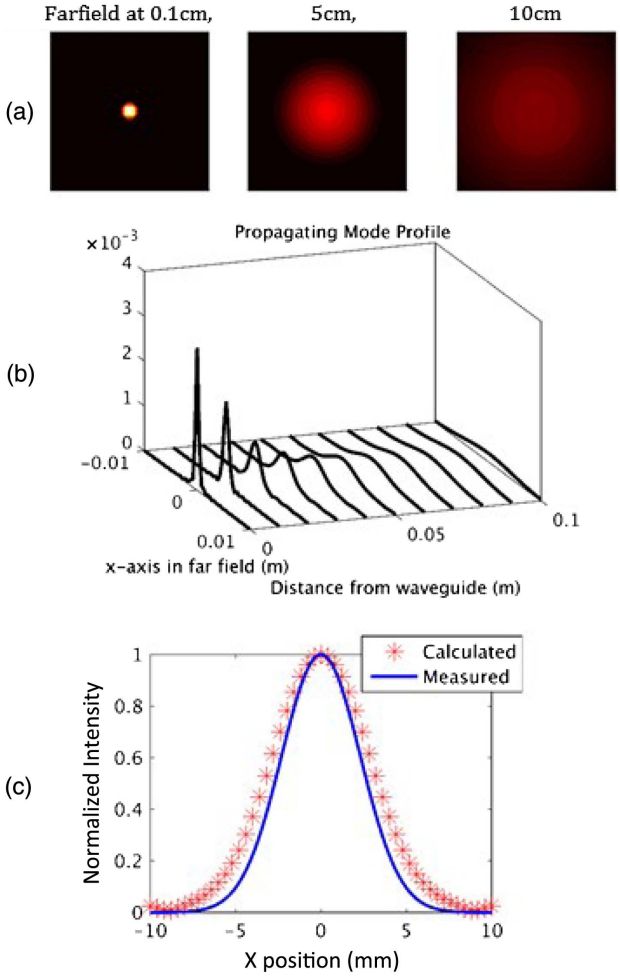

Fig. 6. (a) Calculated THz mode profile at different positions in the far field. (b) Mode profile propagating in free space at 0.32 THz. (c) Measured beam shape at 0.32 THz compared to calculated beam shape at 0.32 THz 6 mm behind the waveguide.

To study the performance of the waveguide further, we performed a loss measurement on waveguide B, the best waveguide based on transmission performance, by measuring the transmission of waveguides 8.6, 6.6, and 3.9 cm long and fitting the results at each frequency. To maintain consistency during these measurements, we aligned all three waveguides using the metal plate as shown in Fig. 3(b), and to avoid problems with the cutting of the waveguide, we printed three different lengths. We also took five measurements for each length of waveguide to reduce the effect of the difference in coupling for each attempt, although coupling can still be a cause for differences between the calculated and measured loss. The comparison between the calculated and measured loss can be seen in Fig. 5. Two antiresonance windows can be clearly seen at roughly the expected spectral position, where the loss becomes approximately 10 times lower than the material bulk loss. Simulations of confinement loss would, however, predict considerably lower loss. One possible explanation for this discrepancy might be due to the light scattering from the 3D-printed surfaces, not accounted for in our simulations [27]. The surfaces of the tubes are considerably rougher in FDM-printed samples than for other 3D-printing methods,

due to the layer thickness of 0.3 mm. Further research into how the surface could be smoothed using annealing or chemical methods could improve the transmission through this type of waveguide.

To use the waveguide for terahertz spectroscopy, it is also useful to know the spot radius of the output beam from the waveguide. To determine the output beam of the waveguide, a free space simulation is performed for the mode at the end of the waveguide [28]. The result of this simulation is compared with the beam profile measured 6 mm behind the waveguide using a knife-edge measurement. The knife-edge measurement is done with the same emitter and detector, but the beam after the knife-edge is focused on the detector using two lenses. The beam width is extracted from the measurements, and a corresponding Gaussian for the beam profile is calculated. It can be seen in Fig. 6 that the calculated and measured beams are very similar, with 15% deviation in the beam width. The discrepancy can be explained by the fitting of the Gaussian beam and the error function to the data. An error of roughly 10% existed in the calculation of the beam width, corresponding to a beam diameter of 9.2 ± 0.9 mm. Although the beam is assumed to be Gaussian, there is probably a small deviation between a Gaussian beam and the output beam from the waveguide. Using this beam profile to calculate the mode propagation in free space, it can be seen from Fig. 6 that the beam is divergent. However, the simulated divergence angle is 3.4°, which is small enough to allow experiments to be conducted in the proximity of the waveguide tip without need of any further lenses. To obtain a collimated beam, a combination of lenses needs to be used. However, due to the increase in transmission, the 3D-printed AR waveguide could be beneficial to use for terahertz transmission.

4. CONCLUSIONS

In this work, we have demonstrated guidance in an AR 3D-printed waveguide using a cheap and simple FDM 3D printer with commercially available low-cost filaments (polycarbonate). Depending on the cladding design, a waveguide can be manufactured within 30 minutes, at low cost. At antiresonance, the transmission is up to 10 times higher through the waveguide than in free space, and with a loss 10 times lower than in the bulk material, showing terahertz guidance in the 3D-printed waveguide across a broad spectral range. This demonstrates how such a simple, cheap, and quickly manufacturable solution can be useful in practice. The guiding of the short AR waveguide (up to 10 cm) could be used in a variety of different tabletop terahertz spectroscopy setups instead of the lens system, which is currently needed to collimate and focus the terahertz beam. Because they are hollow fibers, they could also be used for gas spectroscopy with a species introduced in the fiber. To create longer waveguides, different commercial FDM printers could be utilized to increase the length that can be printed, or a preform could be printed and drawn down into a longer waveguide. Further improvements could be achieved by smoothing the 3D printed surface of the waveguide, for example by annealing and/or chemical treatment, and by using lower loss polymers such as TOPAS.

Funding. Engineering and Physical Sciences Research Council (EPSRC) (EP/N00762X/1); H2020 European Research Council (ERC) (682724).

REFERENCES

1. D. H. Auston, K. P. Cheung, and P. R. Smith, "Picosecond photoconducting hertzian dipoles," Appl. Phys. Lett. **45**, 284–286 (1984).
2. M. C. Beard, G. M. Turner, and C. A. Schmuttenmaer, "Terahertz spectroscopy," J. Phys. Chem. B **106**, 7146–7159 (2002).
3. W. Withayachumnankul and M. Naftaly, "Fundamentals of measurement in terahertz time-domain spectroscopy," J. Infrared, Millimeter, Terahertz Waves **35**, 610–637 (2014).
4. B. M. Fischer, M. Walther, and P. U. Jepsen, "Far-infrared vibrational modes of DNA components studied by terahertz time-domain spectroscopy," Phys. Med. Biol. **47**, 3807–3814 (2002).
5. D. W. Vogt and R. Leonhardt, "3D-printed broadband dielectric tube terahertz waveguide with anti-reflection structure," J. Infrared, Millimeter, Terahertz Waves **37**, 1086–1095 (2016).
6. B. You and J.-Y. Lu, "Remote and *in situ* sensing products in chemical reaction using a flexible terahertz pipe waveguide," Opt. Express **24**, 18013–18023 (2016).
7. N. Laman, S. S. Harsha, and D. Grischkowsky, "Narrow-line waveguide terahertz time-domain spectroscopy of aspirin and aspirin precursors," Appl. Spectrosc. **62**, 319–326 (2008).
8. G. Trichopoulos and K. Sertel, "Polarimetric Terahertz Probe for Endoscopic Assessment of Malignancies," in *IEEE International Symposium Antennas and Propagation & USNC/URSI National Radio Science Meeting* (Institute of Electrical and Electronics Engineers Inc., 2015), Vol. 2015-October, pp. 730–731.
9. D. Jahn, M. Weidenbach, J. Lehr, L. Becker, F. Beltrán-Mejía, S. F. Busch, J. C. Balzer, and M. Koch, "3D printed terahertz focusing grating couplers," J. Infrared, Millimeter, Terahertz Waves **38**, 708–716 (2017).
10. G. P. Williams, "Filling the THz gap—high power sources and applications," Rep. Prog. Phys. **69**, 301–326 (2006).
11. S. Busch, M. Weidenbach, M. Fey, F. Schäfer, T. Probst, and M. Koch, "Optical properties of 3D printable plastics in the THz regime and their application for 3D printed THz optics," J. Infrared, Millimeter, Terahertz Waves **35**, 993–997 (2014).
12. A. Argyros, "Microstructures in polymer fibres for optical fibres, THz waveguides, and fibre-based metamaterials," ISRN Opt. **2013**, 785162 (2013).
13. S. Atakaramians, S. A. Vahid, T. M. Monro, and D. Abbott, "Terahertz dielectric waveguides," Adv. Opt. Photon. **5**, 169–215 (2013).
14. C. M. Smith, N. Venkataraman, M. T. Gallagher, D. Mueller, J. West, N. Borrelli, D. Allan, and K. W. Koch, "Low-loss hollow-core silica/air photonic bandgap fibre," Nature **424**, 657–659 (2003).
15. F. Poletti, "Nested antiresonant nodeless hollow core fiber," Opt. Express **22**, 23807–23828 (2014).
16. E. Canessa, C. Fonda, and M. Zennaro, *Low-cost 3D printing for Science, Education and Sustainable Development*, 1st ed. (ICTP—The Abdus Salam International Centre for Theoretical Physics, 2013).
17. A. I. Hernandez-Serrano and E. Castro-Camus, "Quasi-Wollaston-prism for terahertz frequencies fabricated by 3D printing," J. Infrared, Millimeter, Terahertz Waves **38**, 567–573 (2017).
18. A. I. Hernandez-Serrano, E. Castro-Camus, and D. Lopez-Mago, "q-plate for the generation of terahertz cylindrical vector beams fabricated by 3D printing," J. Infrared, Millimeter, Terahertz Waves **38**, 938–944 (2017).
19. J. Yang, J. Zhao, C. Gong, H. Tian, L. Sun, P. Chen, L. Lin, and W. Liu, "3D printed low-loss THz waveguide based on Kagome photonic crystal structure," Opt. Express **24**, 22454–22460 (2016).
20. A. Cruz, V. Serrão, C. Barbosa, M. Franco, C. Cordeiro, A. Argyros, and X. Tang, "3D printed hollow core fiber with negative curvature for terahertz applications," J. Microwaves, Optoelectron. Electromagn. Appl. **14**, SI45–SI53 (2015).
21. L. D. van Putten, E. N. Fokoua, S. M. A. Mousavi, W. Belardi, S. Chaudhuri, J. V. Badding, and F. Poletti, "Exploring the effect of the core boundary curvature in hollow antiresonant fibers," IEEE Photon. Technol. Lett. **29**, 263–266 (2017).
22. M. Naftaly and R. E. Miles, "Terahertz time-domain spectroscopy for material characterization," Proc. IEEE **95**, 1658–1665 (2007).

23. F. Poletti, J. R. Hayes, and D. Richardson, "Optimising the performances of hollow antiresonant fibres," in *37th European Conference and Exposition on Optical Communications* (Optical Society of America, 2011), paper Mo.2. LeCervin.2.
24. Laserquantum, "Laser quantum, tera-sed," 2017, http://www.laserquantum.com.
25. Menlosystems, "Terahertz antennas and components," 2017, http://www.menlosystems.com/.
26. L. van Putten, J. Gorecki, E. Fokoua, V. Apostolopoulos, and F. Poletti, *Data for '3D Printed Polymer Antiresonant Waveguides for Short Range Terahertz Applications'* (2018).
27. Z. Wang, H. Wu, X. Hu, N. Zhao, Q. Mo, and G. Li, "Rayleigh scattering in few-mode optical fibers," Nature **6**, 35844 (2016).
28. M. Born and E. Wolf, *Principles of Optics: Electromagnetic Theory of Propagation, Interference and Diffraction of Light* (Pergamon, 1959).